FAÇADE PHOTOMETRICS: LUMINANCE DISTRIBUTION ANALYSIS THROUGH BUILDING SKINS

Azadeh Omidfar Sawyer
University of Michigan
aomidfar@post.harvard.edu

Abstract

This paper presents a novel technique to evaluate how building façades propagate light into interior spaces. Just as electric light photometry charts the luminous intensity around a light fixture, Façade Photometry, a term coined by the author for the method introduced in this paper, uses annual simulations and localized weather data to create temporally based luminance distributions. This photometric chart is a unique signature of a particular façade design located in a specific climate in a specific orientation. This method seeks to provide designers the ability to more easily compare the performance of complex and intricate glazing and daylight control systems.

Current methods of obtaining annual luminance values require the collection of High Dynamic Range (HDR) images, an inefficient and time-consuming task; far from optimized for use by the design community. The method proposed in this paper uses a bi-directional measurement of daylight received by digital sensors arranged hemispherically in a black room, aimed at the façade. The results provide data on spatial luminance distribution, vertical eye illuminance distribution, luminance contrast, and glare index from different gazing angles. While further analysis of the method and comparison to human perception is necessary in order to understand the meaning behind the results, the method has the potential to become a streamlined tool to further aid designers in the pursuit of designing highly energy efficient and beautiful spaces.

Introduction

Since the first light survey in an interior space in 1865, we have progressed significantly in our understanding of "good" daylighting in buildings (Ashdown, 2014). Our metrics and simulation tools have of course evolved in parallel. The Daylight Factor (DF), initially introduced in 1895, was followed by the Lumen Method in 1928, understanding luminance distributions in 1942, and the Daylight Glare Index (DGI) in 1950. In 1989 Daylight Autonomy was introduced, then Useful Daylight Illuminance (UDI) in 2005, and recently Spatial Daylight Autonomy (sDA) and Annual Solar Exposure (ASE) in 2012 (John Mardaljevic and Christoffersen 2016; Kota and Habrel 2009; Hopkinson 1963; Peterson 2015; Nabil and Mardaljevic 2006). Clearly there has been a trajectory of achievement in evaluating and simulating natural light. However, most of these metrics, aside from glare studies, rely on measuring daylight quantity on a horizontal working plane approximately 2.5' (0.762m) above the floor at desk level. The most widely used metrics for assessing daylight have continued to rely on assessing the horizontal working plane, even though most occupant work is now conducted on computers with vertical illuminated screens.

Building façade geometry or shading systems can have a dramatic effect on the distribution, directionality and intensity of daylight entering a space, yet commonly used metrics have difficulty accounting for these effects. In addition to these shortcomings, most of the current metrics overlook the inherent dynamic nature and variability of daylight through building façades (Rockcastle and Andersen 2013). Measurements on a horizontal plane cannot possibly illustrate all the lighting characteristics of a façade design. For example, two wildly different façade designs could produce similar daylight autonomy distributions.

Therefore, in order to understand the behavior of daylight through different façade designs, a method that measures the transmission, intensity and distribution of light through the façade is necessary. Façade Photometry introduced and discussed in this paper can measure the luminance distribution of light and it can further be used to understand the correlation between daylight distribution and the room occupants' visual experiences, satisfaction and preferences.

Common Daylight Metrics

Various daylighting metrics exist to guide designers by providing required light levels as needed for a given task and eliminating visual discomfort associated with glare. While available metrics and indices provide valuable information about a space, they all possess some limitations and inadequacies. For example, the most commonly used metric in lighting design is the Daylight Factor, which is defined as the percentage of outdoor illuminance E that falls on the indoor work plane (Hopkinson 1963). Though this is a simple and sometimes useful metric to quickly evaluate illuminance values on a working plane, it does not account for a specific climate nor does it factor in the effect of direct sun exposure, orientation and potential glare (J. Mardaljevic, Heschong, and Lee 2009). This is not to say that DF is not useful and should not be utilized, but to emphasize the importance of understanding the information each metric provides and each metric's shortcomings. If the goal is to quickly

assess the potential amount of light in a space, then DF can be useful; however, if the exact amount of daylight as it relates to the building orientation and climate is important, then other annual climate-based metrics, such as sDA or UDI, should be considered as they provide a more accurate assessment of horizontal illuminance.

These lighting metrics, when used in computer-based simulation approaches, can be divided into two categories, each of which express unique luminous qualities: 1) illuminance and luminance and 2) point-in-time and annual calculations. Task-based metrics rely on illuminance levels on a horizontal plane typically modeled at desk level, while visual comfort metrics typically assessing glare rely on luminance or luminance contrasts in the field of view. Luminance-based metrics can identify localized contrast in addition to average or background luminance values and overall brightness. Currently, the most widely used method to obtain luminance measurements is the rendering of HDR images of a particular view for a specific moment in time and analyzing and post-processing the image to obtain the luminance values of the environment. Rendering hourly HDR images, i.e. for the 8760 hours of the year, and analyzing/post-processing each image to obtain the luminance values are not efficient, economical or effective. In 2009, Wienold proposed a method based on DGP using illuminance values at the eye level as well as simplified HDR images for each hourly time-step. A DGP value is ultimately extracted which did not exceed more than 5% of the usage time. This method is also implemented in the draft of the European standard "Daylight of buildings" prEN17037. Although this method uses a very efficient luminance based evaluation method, the calculation for several viewpoints and viewing directions with this method is very time consuming (Wienold 2009a).

Other newly introduced methods such as the BSDF (3-phase and 5-phase) discussed by Andy McNeil (McNeil 2014) have the capability to characterize light transmission, reflection and directional distribution of the façade. However, systems that are inhomogeneous, such as the Voronoi system used in this study, cannot be easily studied using any BSDF, either measured or calculated using genBSDF. This is because the BSDF and also BTDF assume that the distribution is constant across the surface of complex fenestration system. There are "tricks" to overcome this limitation, however, this particular constraint along with its complex nature is the reason this method was not utilized in this research study.

As luminance is most closely related to the way in which the human eye perceives brightness and contrast, to assess the daylight distribution as perceived by occupants, luminance and vertical eye illuminance measurements become the key variables in assessing the performance of the façade and its effect on the environment it encloses. Previous research studies have also shown the correlation between vertical illuminance at eye level and glare perception (Wienold 2009b). Thus, this study focuses on the ways in which luminance distribution can be digitally and efficiently calculated.

Building Façades Evaluation: Far-Field vs. Near-Field Photometry

In the field of photometry, light is measured in terms of its perceived brightness to the human eye, which is different than measuring radiant energy in terms of absolute power (Bass 1995). Because photometry is a polar measurement of candela values, the luminous intensity of a light source from all angles is defined. There are various apparatuses, meters and techniques to physically measure the luminous flux and intensity of luminaires. For example, to assess the performance of a luminaire or a light fixture, engineers typically use either the far-field photometric measurement procedure or near-field measuring techniques. Far-field requires the photometer to be at a distance that is roughly five times greater than the maximum projected dimension of the luminaire. In near-field photometry, the meter can be at a distance of roughly the maximum width of the luminaire (Ashdown 1993). Employing photometric data from a large distance, i.e. appropriate to the far-field measurements, evaluates the fixture as a point source which is photometrically homogenous (Ngai 1987). It can be argued that a building façade can be viewed as a light fixture, but the light source, the sun, is dynamic. Therefore, neither far-field nor near-field methods can be used for assessing the performance of a building façade system.

It is obvious that a building façade cannot be viewed either as a point source or as a homogenous structure, and since the sensors need to be at the observer position, the rule of far-field photometry cannot be utilized. On the other hand, near-field allows us to calculate light intensity and distribution considering the fixture, as a collection of components with unique photometric behavior (Ngai 1987). The difficulty with the near field measurements rule in measuring façade performance, is the location of the sensors in relation to the fixture. Because the façade is a large area source, to have the sensors at a distance that is equal to the width of the fixture it would require the sensors to be far away which would not capture the light distribution accurately. It is also important to note here that neither method has ever been used to assess shading systems or building façades in general.

Methodology

In order to measure the luminance distribution of each façade design, it was necessary to develop a digital technique to simulate annual luminance distribution that could later be used for subjective analysis. A physical measuring technique in near-field photometry has been previously developed using an aperture- type photometer. This type of meter measures the luminous flux contained within a specific solid angle and an area of a sensor (Ashdown 1993).

This research project used the specifications of the size of the meter and its projected field of view (FOV) as described by Ashdown (2013). However, since the relationship between the FOV of the façade and occupants' visual experience has never been researched and is unidentified, two different FOVs have been tested

in this study: a narrow FOV with high-frequency information and a wide FOV with low-frequency information. The overarching goal of the research, of which this article is the first phase, is to see which datasets correlate with the observer preferences.

For the simulation of the luminance distribution, the bi-directional simulation technique was used. The aperture-type meter illustrated in Figure 3 measures an approximation of luminance due to its finite field of view. This technique calculates the luminance transmitted or reflected off various complex façade systems at an equal solid angle as viewed from the interior space. Each digital sensor used measures the luminance distribution on an imaginary hemispherical surface located in the room with the concave side facing the façade.

This photometric test reports the luminous intensity distribution, luminance and illuminance peaks, and averages. It also provides vertical eye illuminance in east, west, north and south directions, as well as vertical eye luminance at every gazing angle. These values can be used to compute glare, contrast, and veiling reflections. The model is developed parametrically, so one has the option of viewing the luminance and vertical eye illuminance distributions dynamically for all the hours of the year.

Software

The first phase of this study required digital models and a validated daylight simulation engine. For this study, detailed digital models of a base case and two case studies were generated in Rhinoceros (Rhino) CAD environment. Rhino is a stand-alone, commercial NURBS-based 3-D modeling tool, developed by Robert McNeel and Associates (McNeel 2010). The custom sensors for the bi-directional measurement technique were developed in Grasshopper. Grasshopper is a graphical algorithm plug-in for Rhino which allows for parametric modeling and scripting. All daylight simulations were performed using DIVA Grasshopper (Jakubiec and Reinhart 2011). The DIVA plug-in supports a series of performance evaluations. Using DIVA for Grasshopper plug-in, the models were exported into the validated Radiance simulation program. All hourly Luminance distribution for each façade has been simulated using both FOVs.

Case Study- Comparing Different Façade Designs

A south facing, double glazed, open plan space was assumed as the test space. The test space measured 12'-0" (3.65m) wide, 18'-0" (5.48m) deep 12'-0" (3.65m) high. For the purpose of this study, the walls, ceiling, and floor of the room were modeled as black with 0% reflectance to eliminate the complications of room surfaces interreflections and to only focus on the effect of façade geometrical patterns. The glazing portion of the façade and each façade system was reduced to a module of 9'-0"x 9'-0" (2.74m x2.74m) to reduce the simulation time. The glass is modeled as a double pane glazing with 80% transmittance. The New York, NY (42.35 N, 71 W) weather file was used for all simulations. Three case studies were analyzed and will be illustrated in this paper: a base case with a double pane glass window devoid of a shading system, a room with a Voronoi shading system and a room with a Horizontal Louvers as shown in Figure 1. Radiance simulation parameters are listed in Table 1. These parameters are utilized to reduce the simulation time while accurately representing the effect of complex fenestration devices. The CIE clear sky condition was used for all simulations in this phase of the study.

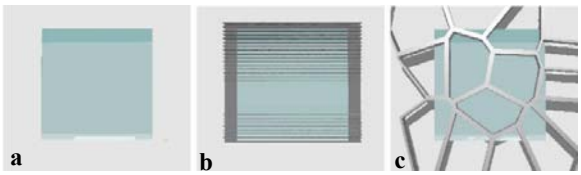

Figure 1- a. base case (glass), b. Horizontal Louvers, c. Voronoi System

Table 1: Radiance simulation parameters

Ambient Bounces	Ambient Division	Ambient Sampling	Ambient Accuracy	Ambient Resolution
4	1500	256	.1	256

Digital Luminance & Vertical Eye Illuminance Meter

As previously mentioned, this bi-directional modeling technique utilizes custom sensors modeled on the concave face of an imaginary hemispherical surface. Each sensor possesses a XYZ coordinate location, viewing directions, and an angle which can be used to assess their field of view (FOV). Different discretization of the surface was tested in this research. The different sensor arrangement ranged from 145 sensors to 1350. The diagrams and the results shown in this paper used a sensor arrangement on a hemisphere subdivided into 36 sections each with 19 sensors which resulted in 684 sensors, at every ~ 5 latitude as shown in Figure 2.

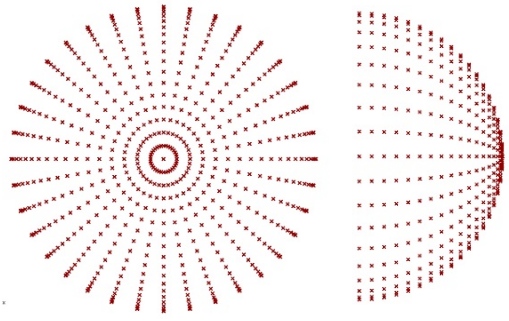

Figure 2- front and side view of the 684-hemispherical sensor arrangement

The network of sensors faces the window and follows the direction normal to the surface of the hemisphere. An aperture-type meter geometry, i.e. a cylindrical shield shown in figure 3 was then developed for each sensor. Following Ashdown's recommendation on the size of the aperture-type meter, two different cylindrical shields were

developed. The first cylindrical shield measures 1.368" (3.47cm) in diameter and 6.84" (17.37cm) in length which provides a FOV of 11.42°.

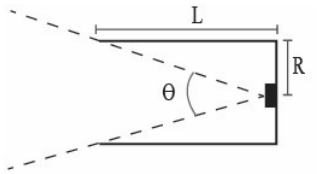

Figure 3- Aperture-type diagram (cylindrical shield)

Field of View (Wide)

$$FOV(\theta) = 2.0 * \tan^{-1}(Radius/Length) \quad (1)$$

$$FOV\ Wide(\theta) = 2.0 * \tan^{-1}(0.684/6.84) = 39.2^{\circ}$$

The second cylindrical shield designed measures 1.368" (3.47cm) in diameter and 1.92" (4.87 cm) in length which provides a FOV of 39.2°.

Field of View (Narrow)

$$FOV\ Narrow\ (\theta) = 2.0 * \tan^{-1}(0.684/1.92) = 11.42^{\circ}$$

With this hemispherical sensor arrangement, each sensor has a field of view measuring the luminance variation of every hour of the year. The concept diagrams shown in figure 4 illustrate three sensor points and the viewing angles as well as the side view of the sensor arrangement and their viewing directions.

As shown in figure 5, the hemisphere is located in the room within close proximity of the façade, roughly 9' (2.74 m) away. The sensors follow the directions normal to the surface of the hemisphere, therefore, the sensors that are closer to the edge of the hemisphere are facing the surrounding walls, away from the façade.

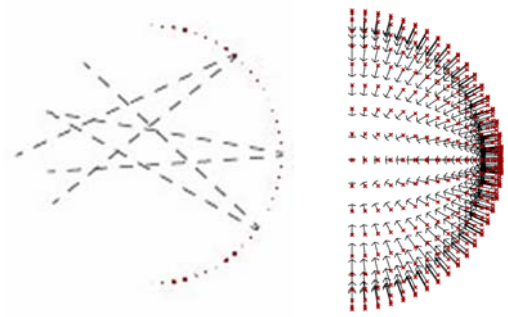

Figure 4- On the left: Concept diagram of the sensors and their viewing angle. On the right: Sensors on the hemisphere and their viewing directions

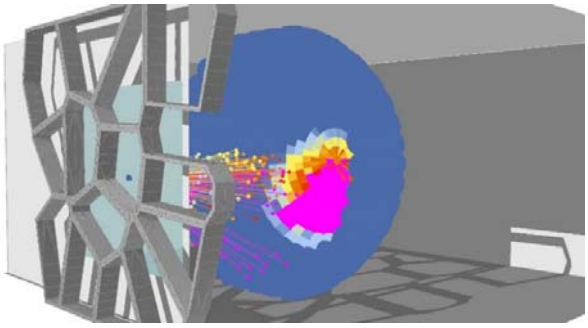

Figure 5- Position of the hemisphere in the room

In this project, because the walls, ceiling and floor are all black, the sensors that are facing the walls do not detect any light reflection, therefore, the measured values are zero. If the walls are modeled with materials other than black, then the sensors will measure the amount of light that reflects off the surrounding wall surfaces.

Illuminance to Luminance Calculations Using Aperture-Type Meters:

Following the equations provided in the IES handbook, luminance values can be calculated and compared to the simulated results. Because the aperture-type meters are following the normal of the hemisphere and the values are not measured horizontally, no corrections will be needed, thus, the following equations can be used to calculate the luminance values of each sensor:

The calculation of the illuminance from a luminance distribution of a hemisphere is defined as:

$$E = \int L \cdot \cos\theta \cdot d\omega \quad (2)$$

for a small aperture type meter this equation can be simplified to:

$$E_{shield} \approx L_{avg} \cdot \Omega_{sheild}$$

This gives:

$$L(avg)=E\ (shield)/\ \Omega(shield)$$

Where θ is ½ of the angle of the cylindrical shield or the FOV.

Thus, for the narrow FOV (11.42°):

$$L=E/(2\pi(1-\cos\ (11.42*\pi/360))$$
$$L=E/0.0312$$

For the wide FOV (39.2°):

$$L= E/\ (2\pi\ (1-\cos\ (39.2*\pi/360))$$
$$L=E/0.379$$

E= Illuminance

L=Luminance

θ= Angular distance from sensor normal to source (Which is zero due to the viewing angle, therefore $\cos\theta = 1$)

Ω=Solid angle of the shield

The aperture-type photometer measures an approximation of luminance due to its finite field of view. Once the values are simulated using DIVA Grasshopper, they are then divided by the solid angle for average luminance as

shown above. The hemispherical sensor arrangement is equivalent to a fisheye lens with a 180-degree field of view, with each sensor having a FOV, which in a sense results in a low-resolution fisheye image.

Results:

The spatial luminance distribution graphs shown in Figures 6-8 illustrate the variability of daylight for every hour captured at each sensor. This visualization is important as the peaks can be easily detected. Since the viewing direction of each sensor is defined, a particular sensor on the hemisphere reading high light levels can be simply highlighted and traced back to a particular region of the façade and adjustments to the geometry can be made. In both the base case and the Voronoi System the light levels vary significantly during the winter months (Figure 6 & Figure 8). The light is more uniform in the room with the Horizontal Louvers; the peaks are significantly lower than the base case and the Voronoi System (Figure 7).

The bi-directional method measures luminance distribution of each façade design. The luminance spatial distributions of each façade design options for December 21st, at 11:30 pm, are shown in Figure 9 and Figure 10. The intensity and the spatial distribution vastly differs among the different options, specifically in the façade option with the Horizontal Louvers (Figure 9b). The Base Case luminance distribution graph illustrates much higher levels (Figure 9a). There is a large influx of light penetration toward the bottom of the room in both the Base Case and the Voronoi System design options (Figure 9a & 9c); this is expected and consistent with the reality due to the sun's position in the sky. The luminance distribution using the Narrow FOV displays a similar pattern of light distribution, with much higher intensity dues to its solid angle (Figure 10). There is a considerable difference between the amount of light and its distribution between the different options, specifically the Horizontal Louvers (Figure 10b).

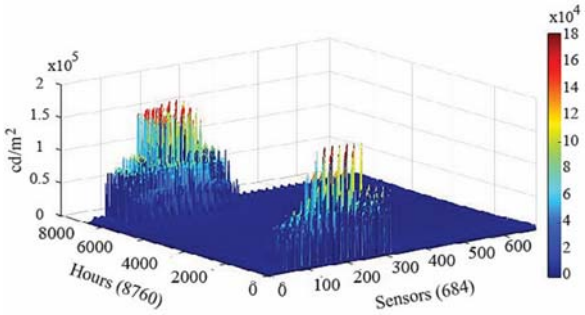

Figure 6- Base case (glass): Luminance distribution using Wide FOV

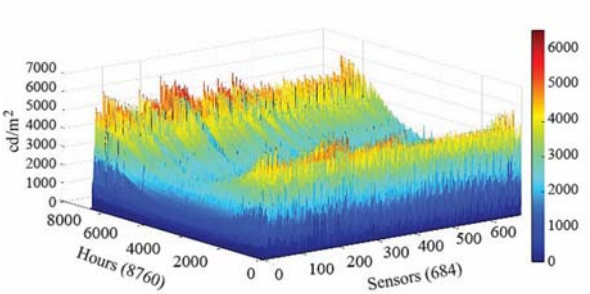

Figure 7- Horizontal Louvers: Luminance distribution using Wide FOV

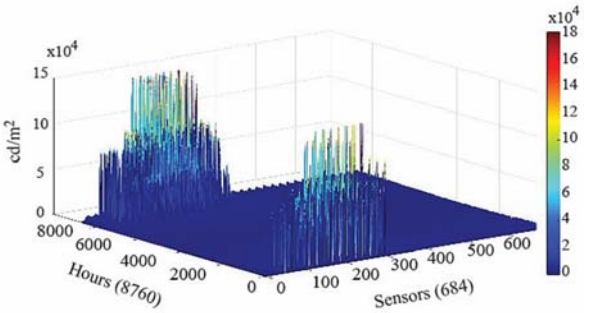

Figure 8- Voronoi system: Luminance distribution using Wide FOV

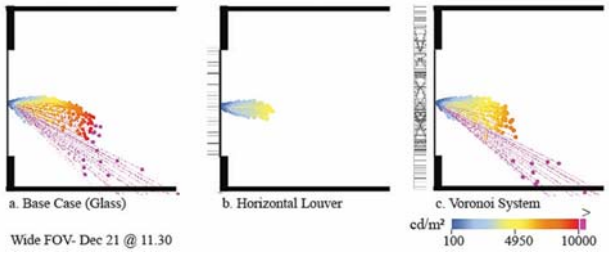

Figure 9- Spatial Luminance distribution of the three case studies using wide FOV.

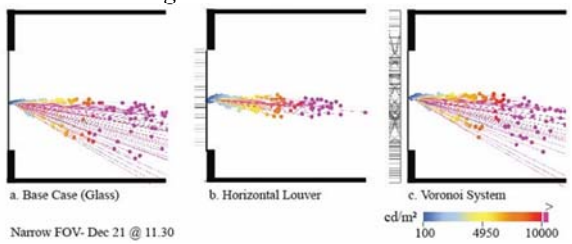

Figure 10- Spatial Luminance distribution of the three case studies using Narrow FOV.

The luminance distribution for a specific time, of both the narrow and wide FOVs, can also be observed at each sensor on the surface of the hemisphere (Figure 11-12). As the sensors toward the perimeter of the hemisphere are directed at the surrounding black surfaces, they are not receiving any direct or reflected light and therefore are diagrammatically presented as dark blue. The Voronoi system shows intense levels of light towards the bottom of the hemisphere (Figure 11c). High levels of light indicate direct light that could cause visual discomfort.

Light levels are reduced in the Horizontal Louvers and the concentration is in the center of the hemisphere (Figure 11b).

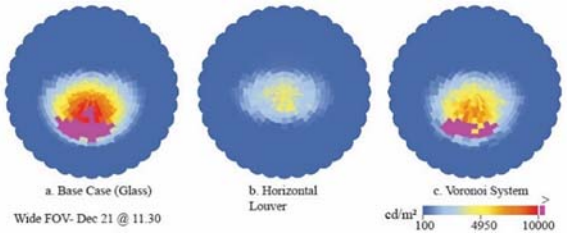

Figure 11- Luminance distribution on the hemisphere, using sensors with wide FOV

The luminance distribution patterns of the narrow FOV shown on the hemispherical diagrams are similar to those from the wide FOV; however, the light levels dramatically increase due to its small solid angle, particularly in the diagram for the Horizontal Louvers (Figure 12b).

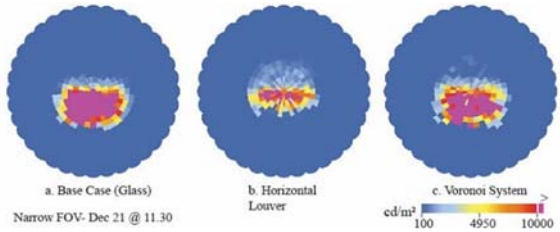

Figure 12- Luminance distribution on the hemisphere, using sensors with narrow FOV

Most designers simulate and analyze only extreme light conditions, generally March, June, September, and December 21st at noon. However, the annual luminance distribution graph of the Voronoi System, using the sensor on the center of the hemisphere illustrates the times that yield higher values and produce conditions that could result in an uncomfortable environment (Figure 15). The HDR images shown are for Dec 21st and June 21st at 12:30 pm (Figure 14 A & B). Fewer light variations are seen in the option with the Horizontal Louvers (Figure 13 &14).

Figure 13- HDR images- Dec 21st @ 12:30

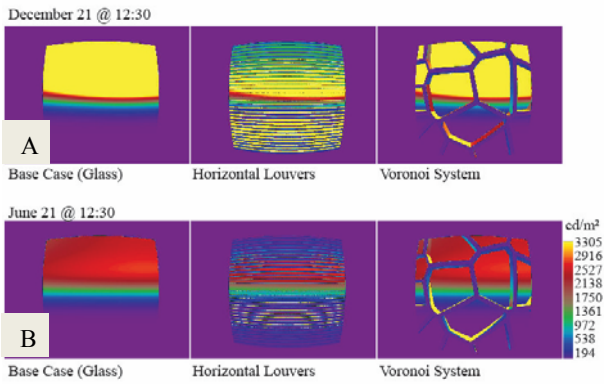

Figure 14- False color analysis of all spaces for Dec and June @ 12:30

Using the hourly graph, outliers can be detected and further analyzed for an additional understanding of the daylight variations in the space. One of the extreme conditions occurring on Nov 9th at 11:30 am is highlighted in the annual luminance distribution graph (Figure 15). Luminance values for that particular day can be viewed and analyzed separately to understand the light variation (Figure 16). An increase in light levels is seen from 6:30 am to 11:30 am, reaching its peak at approximately 7,083 cd/m^2, with a rapid decrease in light levels from 11:30am to 12:30 pm (Figure 16).

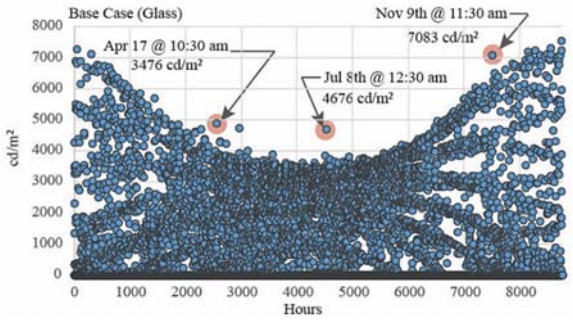

Figure 15- Annual luminance distribution of the Base Case System, using the sensor on the center of the hemisphere, perpendicular to the window.

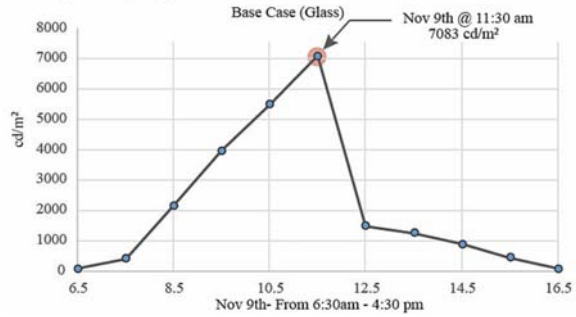

Figure 16- Further hourly analysis of the light behavior using Base Case for Nov 9th

The subdivision and the arrangement of the sensors provide flexibility for detailed analysis of each segment. Figure 17 of the Voronoi System and Figure 18 of the Horizontal Louvers demonstrate the luminance values

received at the sensors with narrow FOV, following the horizontal and vertical ribs in the center of the hemisphere. The graphs highlight the distribution and the daylight variability of each month, and clearly illustrate the peak values. Large peaks occur in the center and bottom of the hemisphere, between 80°-100° horizontally (Figure 17 A) and 60°-100° vertically (Figure 17 B). For December 21st at 11:30 pm, the highest values are seen in December and October respectively.

Utilizing the narrow FOV dataset, less light variation is seen in the Horizontal Louvers (Figure 18). For December 21st at 11:30 pm, the high values occur in December and October (Figure 18). The highest light level in the Voronoi System is on the vertical rib at 60°, whereas in the Horizontal Louvers the highest value is on the horizontal rib around 80°.

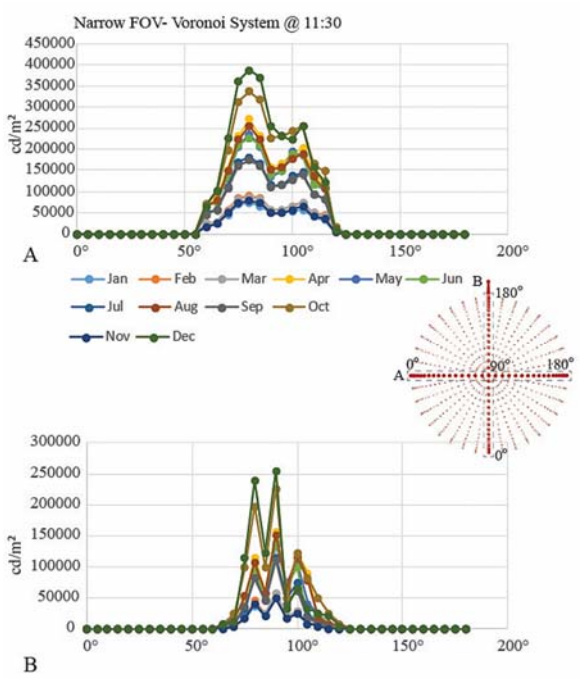

Figure 17- Graph A: Luminance values of the Voronoi System, measured by each sensor on the horizontal rib of the hemisphere. Graph B: Luminance values of the Voronoi System measured by each sensor on the vertical rib of the hemisphere

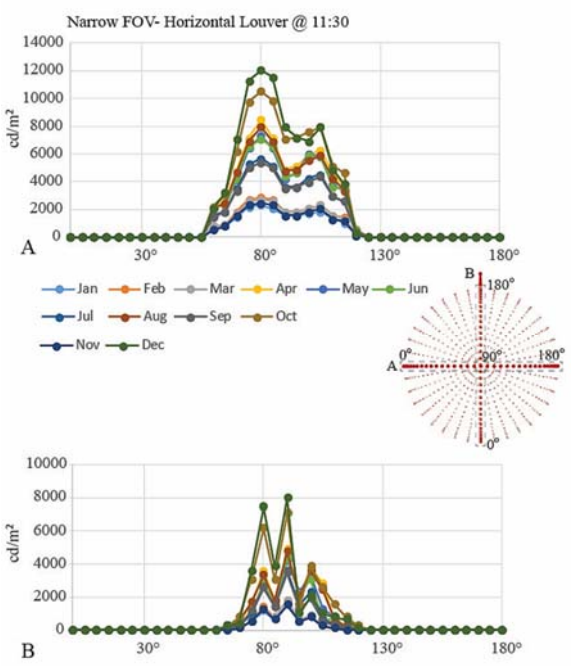

Figure 18- Graph A: Luminance values of the Horizontal Louvers, measured by each sensor on the horizontal rib of the hemisphere. Graph B: Luminance values of the Horizontal Louvers measured by each sensor on the vertical rib of the hemisphere

As the field of view changes, the luminance values change as well. Selecting a limited set of sensors, particularly the ones facing the Base Case façade, the luminance values for December 21st at 11:30 using wide FOV is compared to the values of the same time using the narrow FOV (Figure 19). As expected, the narrow FOV has larger peaks; this is due to the smaller solid angle. Additionally, it is important to understand that there are times where the narrow FOV only "sees" the sky whereas the wide FOV will average between the sky and the shading system, therefore the pattern is accurate and expected. The average hourly luminance values for Dec 21st are shown for both the wide and Narrow FOV and a similar pattern is observed (Figure 20). The highest peaks occur on sensors 127 and 146, which are on the north-east quadrant of the hemisphere closer to the center.

Though the Wide and Narrow FOV data generally follow the same pattern, further analysis, including subjective surveys, is needed to elucidate which datasets would correlate more closely with the occupants' visual preferences and satisfaction.

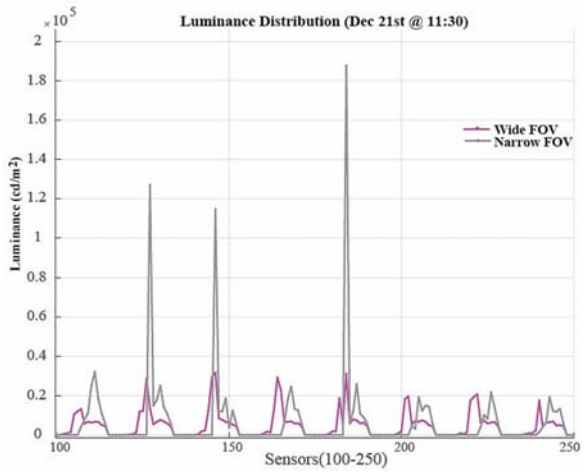

Figure 19- Base Case (glass): Hourly luminance values of sensors 100-250 for Dec 21st at 11:30am using both narrow and wide FOV

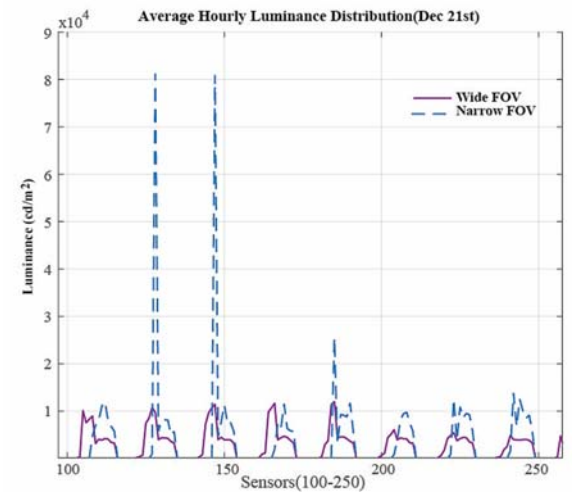

Figure 20- Base Case (glass): Average hourly luminance values of sensors 100-250 for Dec 21st using both narrow and wide FOV

Discussion & Future works:

The Façade Photometric method can be used to assess the light distribution propagating from a façade, as well as highlighting which areas of a façade design could be adjusted for a better performance. For example, if the Voronoi System is aesthetically desired, then this system could be adjusted to reduce visual discomfort associated with glare. However, in addition to quantitative measurements, light quality must be evaluated. Shadow patterns created by building façades can dramatically affect the visual comfort of the users. Unfortunately, there are no known studies on the effect of façade geometry on daylight quality and spatial distribution of daylight over time. The Façade Photometric method has the potential to better our understanding of daylight dynamics, and to connect it with the façade design process. More studies are required to find ways to consolidate the data into a more meaningful representation.

Further examination of the values associated with glare, and subjective analysis to correlate the data to occupants' preferences and satisfaction will be explored in subsequent research analyses. The overarching goal is to develop a metric that correlates with the room occupants' visual experience and satisfaction, with the lighting, and to provide designers a concise method of assessing façade designs against a baseline using simple, intuitive logics.
Since all simulations in this study are conducted using DIVA, which uses Radiance and Daysim, there are limitations that need to be noted here. First: because the initial calculations are illuminance based calculations in DIVA, specular reflections of the sun cannot be detected. This can be a major issue if the shading system has specular characteristics and if the values are used for glare analysis. Since none of the shading systems are specular in this study, this limitation was not an issue in this particular research. Second, Daysim uses a sun discretization of roughly 65 sun positions. This discretization and interpolation of the sun positions could lead to underestimated values for certain shading systems. Due to the sun-interpolation, high luminance values can be observed for more than one cone at the same timestep as well. These problems will be studied and addressed in the next phase of the research.

Conclusion:

Current lighting metrics do not adequately represent the spatial distribution of daylight as affected by building façades. The desire to bring natural light in spaces is not merely for the purpose of completing specific tasks, therefore, it is critical to find ways to evaluate daylight distribution as it relates to the perceived brightness, visual comfort, and ambiance. Building façade geometry dramatically affects daylight directionality, distribution and intensity. This paper has presented a new approach to measuring luminance, and described a technique to calculate luminance distributions using different FOVs. The results show that the Façade Photometry technique provides annual luminance values from different gazing angles and directions much faster than other techniques discussed in this paper. The simulation provides the peaks, luminance distribution, and luminance contrast, which can be used to calculate visual discomfort associated with glare. With further refinement, the process has the potential to provide designers a fundamentally new metric with which to assess design options.

Acknowledgements:

I would like to thank my advisor, Mojtaba Navvab, for his tremendous support. A special thank you to Alstan Jakubiec, Ian Ashdown, Jan Wienold and Dan Weissman for their continuous advice and guidance in this research.

References:

Ashdown, Ian. 1993. “Near-Field Photometry: A New Approach.” *Journal of the Illuminating Engineering Society* 22 (1): 163–80. doi:10.1080/00994480.1993.10748029.

Bass, Michael. 1995. “Devices, Measurements and Properties.” In *Handbook of Optics*, 2nded., 24–40. McGraw-Hill.

Hopkinson, Ralph Galbraith. 1963. *Architectural Physics: Lighting*. London: H. M. Stationery Off.

Jakubiec, J Alstan, and Christoph F Reinhart. 2011. “Diva 2 . 0 : Integrating Daylight and Thermal Simulations Using Rhinoceros 3D , Daysim and Energyplus.” In *Proceedings of Building Simulation*, 2202–9. Melbourne.

Kota, Sandeep, and Jeff Habrel. 2009. “Historical Survey of Daylighting Calculations Methods and Their Use in Energy Performance Simulations.” In *International Conference for Enhanced Building Operations*. Energy Systems Laboratory, http : / /hdl .handle .net /1969 .1 /90845.

Mardaljevic, J., L. Heschong, and E. Lee. 2009. “Daylight Metrics and Energy Savings.” *Lighting Research and Technology* 41 (3): 261–83. doi:10.1177/1477153509339703.

Mardaljevic, John, and J. Christoffersen. 2016. “‘ Climate Connectivity ’ in the Daylight Factor Basis of Building Standards.” *Building and Environment* 113: 200–209. doi:10.1016/j.buildenv.2016.08.009.

McNeel, Robert. 2010. “Rhinoceros: Nurbs Modeling for Rhino.” Robert NcNeel and Associates. Available From www.rhino3d.com.

McNeil, Andy. 2014. “BSDFs, Matrices and Phases.” In *13th International Radiance Workshop*, 158. London: Radiance-Online.org. https://www.radiance-online.org/community/workshops/2014-london/presentations/day1/McNeil_BSDFsandPhases.pdf.

Nabil, Azza, and John Mardaljevic. 2006. “Useful Daylight Illuminances: A Replacement for Daylight Factors.” *Energy and Buildings* 38: 905–13. doi:10.1016/j.enbuild.2006.03.013.

Ngai, P.Y. Y. 1987. “On Near-Field Photometry.” *Journal of the Illuminating Engineering Society* 16 (2): 129–36. doi:10.1080/00994480.1987.10748693.

Peterson, Nicole L. 2015. “The Space Between Research and Practice : A Critical Evaluation of Computer-Based Lighting Metrics.” Master’s Thesis, University of Washington, ProQuest (1599904). https://digital.lib.washington.edu/researchworks/handle/1773/33446.

Rockcastle, Siobhan, and Marilyne Andersen. 2013. *Annual Dynamics of Daylight Variability and Contrast A Simulation-Based Approach to Quantifying Visual Effects in Architecture*. 1sted. Springer London. doi:10.1007/978-1-4471-5233-0.

Wienold, Jan. 2009a. “Daylight Glare in Offices.” PhD Diss, Fraunhofer ISE (TH). http://publica.fraunhofer.de/documents/N-141457.html.

———. 2009b. “Dynamic Daylight Glare Evaluation.” In *International Building Performance Simulation Asscociation (IBPSA)*, 944–51. Glasgow. http://www.ibpsa.org/proceedings/BS2009/BS09_0944_951.pdf.